CHAPTER 6

X-RAY NOVA SCORPII 1994 (=GRO J1655-40)

And everything under the Sun is in tune,
But the Sun is eclipsed by the Moon.
(Pink Floyd 1973)

6.1. THE OBJECT

GRO J1655-40 (=X-Ray Nova Scorpii 1994) was discovered as a new X-ray source on July 27, 1994 (Zhang et al. 1994, Harmon et al. 1995a) with the BATSE instrument mounted on the Compton Gamma-Ray Observatory satellite. The intensity of the emission in the 20÷100 keV was of about 1 Crab (Zhang et al. 1994). The analysis of the X-ray spectrum, made by Wilson et al. (1994), allowed the classification of the object as a SXT and as a BHC. The high-energy X-ray spectrum showed a power-law shape with spectral index α varying between 2.5 and 3.1 during the outburst (Harmon et al. 1995a). Crary et al. (1996) searched for the presence of fast X-ray light curve variations at the beginning of the outburst but they found nothing significant.

The optical counterpart was found by Bailyn et al. (1995a) as a 14.2 *V*-magnitude star, with strong Balmer, He I, He II and N III emission lines superposed to a rather reddened continuum (these authors computed a color excess $E(B-V)$ = 1.15 mag from the interstellar Na doublet in absorption located at 5890 Å). They also identified on an archive plate the precursor of the X-ray Nova as a star with V = 17, which led to hypothesize the presence of a subgiant secondary star, rather than a Main Sequence one, in this system. The coordinates of the optical counterpart of this X-ray Nova are (J2000): $\alpha = 16^h\ 54^m\ 00^s.137$; $\delta = -39°\ 50'\ 44''.90$ (Bailyn et al. 1995a).

Radio observations (Hjellming & Rupen 1995, Tingay et al. 1995) have shown the presence of radio jets, similar to those exhibited by active galactic nuclei, though on a much smaller scale. This is a unique feature for a SXT. Some important parameters of this binary system, such as the distance and the inclination (≈3.2 kpc and ≈85° respectively, according to Hjellming & Rupen 1995), were derived by studying the structure of the radio jets. A high inclination for the system is also suggested by Bailyn et al. (1995a), who probably observed, on August 17, 1994, a variation likely due to an eclipse in both the *V* filter and *V-I* color index light curves.

During the six months following the first outburst, the object experienced two additional strong X-ray brightenings (Harmon et al. 1995a), thus showing an outstanding behaviour among the other SXTs, which generally present only one primary maximum at the beginning of the outburst. The radio light curve also presented secondary maxima in correspondence of the X-ray outbursts, indicating a clear correlation between the matter accretion onto the compact object and the jet phenomenon (Harmon et al. 1995a, Meier 1996).

Further X-ray outbursts have been detected during 1995 (Harmon et al. 1995b, Alexandrovich et al. 1995, Harmon et al. 1995c, Wilson et al. 1995, Harmon et al. 1995d, Harmon et al. 1995e, Sazonov & Sunyaev 1995a), the last one peaking on August 17, 1995 (Sazonov & Sunyaev 1995b, Zhang et al. 1995). This indicates that more than one year after the beginning of the high-energy activity, the nova was still well far from quiescence. Furthermore, Zhang et al. (1995) noticed that the X-ray maxima seem to recur with a periodicity of ~120 days.

A restart of the X-ray activity has been noticed in the late April 1996: Remillard et al. (1996) reported that the object has reached an X-ray flux of 1.5 Crab, comparable with those of the previous X-ray maxima. At the beginning of July 1996, Harmon et al. (1996a) reported that the object was still showing a high X-ray emission level (~1 Crab), while Harmon et al. (1996b) remarked the presence of a new X-ray luminosity increase at the end of October 1996.

Besides this X-ray activity in the last two years, a similar behaviour was observed both in the radio (Hunstead & Campbell-Wilson 1996) and in the optical (Orosz et al. 1995, Horne et al. 1996) in coincidence with the X-ray maxima.

Spectrophotometric observations in the optical band have been performed by Bailyn et al. (1995b) during the period March 18 - May 3, 1995, while the source was in a low state of activity (the mean *V* magnitude was 16.4). These authors found a spectroscopic orbital periodicity of 2.601 ± 0.007 days and a mass function of 3.16 ± 0.15 $M_\odot$ for the compact object. This value labels by default GRO J1655-40 as a BHC. Moreover, as supposed by Bailyn et al. (1995a), the secondary star is most probably a yellow subgiant of spectral type F5 IV. This system is then very likely compsed of a ~5 $M_\odot$ BH and by an evolved ~1 $M_\odot$ secondary. The *V*-band photometry data by Bailyn et al. (1995b) show a very wide primary eclipse and a smaller scondary eclipse (Fig. 6.8), thus confirming the high inclination of this system. Also, these authors note that the *V* data seem to indicate that the periodicity of the light curve is slightly longer than that measured spectroscopically, thus suggesting some sort of activity of the disk (i.e. hot spots or superhumps).

Finally, Brandt et al. (1995) found that the velocity of the center of mass of this binary system, found by Bailyn et al. (1995b) to be -150 ± 19 km s^{-1}, is fairly high compared to the velocities of the other BHXNe, and analyzed several scenarios for the genesis of a high-velocity BH binary.

In this paper spectroscopic observations made partly during the early outburst phases and partly during the decline are presented. The analysis of the continuum and of the main emission lines will show the presence of a periodicity which is the half of that found by Bailyn et al. (1995b). Particularly, in Sect. 6.4 an explanation of this result will be given, along with the physical interpretation of the evolution of the spectra from the light maximum to the decline. An explanation to the anomalous extension of the primary eclipse will also be given and a possible scenario for the system will be depicted.

6.2. THE OBSERVATIONS

The observations, which were centered on spectroscopy, were performed partly during the first stages of the outburst (August 1994) and partly during the decline (March 1995). The spectra were all taken at ESO telescopes in La Silla during two different runs (see the upper part of the observations journal reported in Table 6.I).

During the first observing run the source was monitored soon after the first X-ray outburst, from August 12 to 15, 1994, using the 1.5m ESO telescope equipped with the Boller & Chivens spectrograph plus CCD (ESO #24, Ford 2048L, pixel size = 15 μm). In total, 40 spectra using grating n° 4 (3500÷9400 Å range), with a dispersion of about 2.8 Å pixel^{-1} were collected.

Table 6.I. The journal of the observations presented in this Chapter. The upper part of the Table lists the spectroscopic data, while the single photometric observation is reported in the lower part

Date	Telescope	Filter or passband	Number of Frames	Exposure times (in minutes)
SPECTRA				
August 12, 1994	1.5 m.	*Grat*4	2	20; 45
August 13, 1994	1.5 m.	*Grat*4	5	15
August 14, 1994	1.5 m.	*Grat*4	18	12
August 15, 1994	1.5 m.	*Grat*4	15	12
March 3, 1995	NTT	#2; *Grat*7	1; 3	10; 20; 40
March 4, 1995	NTT	*Grat*7	9	10; 15; 20; 25
IMAGING				
March 3, 1995	NTT	*R*	1	1

The second observing run was performed 7 months later, on March 3-4, 1995, shortly after a period of strong X-ray activity (Alexandrovich et al. 1995). For these observations the NTT telescope and the EMMI spectrophotometer equipped with the Tektronix CCD TK2048EB (ESO #36, pixel size = 24 μm) were used. With this setup 13 spectra were obtained: one in mid-resolution mode with the grism #2 (3900÷9600 Å range), and the other 12 in the high-resolution mode with the grating 7 (with a wavelength range of 1180 Å) centered at about 6000 Å. The dispersions were 2.8 Å pixel^{-1} and 0.65 Å pixel^{-1}, respectively.

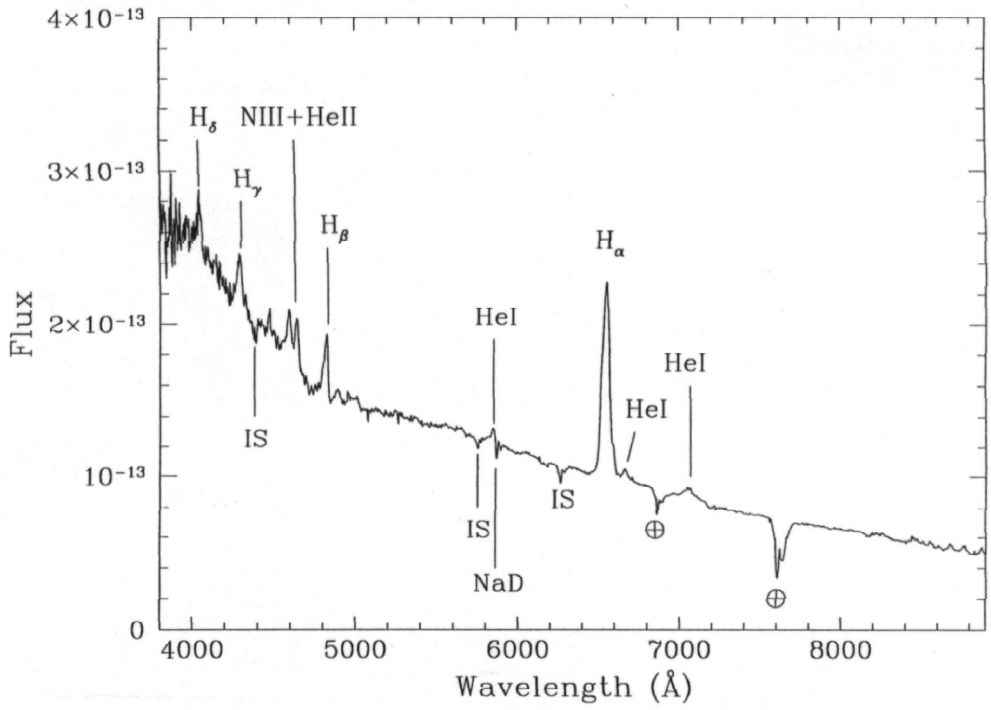

Fig. 6.1. Mean of the outburst spectra taken during the August 1994 run. The main features are indicated and described in the text. A color excess $E(B\text{-}V) = 1.13$ was used to correct for interstellar reddening. Fluxes are in ergs cm^{-2} s^{-1} Å^{-1}.

A single *R*-band image of GRO J1655-40 was also obtained on March 3, 1995 (lower part of Table 6.I) with NTT plus EMMI. This imaging observation, processed in the standard way (see Chs. 4 and 5) showed the star at $R = 14.33 \pm 0.03$ on that night.

6.3. DATA REDUCTION AND ANALYSIS

All the spectra have been at first corrected with standard procedures for bias and flat field and then extracted and processed with the IRAF package. Wavelength calibrations were made by means of He-Ar lamps, and flux calibrations were performed using the spectroscopic standards LTT 7379, LTT 377 and LTT 9239 for the spectra of the August 1994 run, and LTT 4364 for those of the March 1995 run.

The EWs of the interstellar 5980 Å (Na I doublet) and the 6613 Å line measured on the high-resolution spectra, by fitting gaussian profiles, result in 2.26 Å and 0.27 Å, respectively. Using the relations between the EWs of these lines and the *B-V* color excess given by Della Valle & Dürbeck (1993) for the NaD doublet, and by Herbig

(1975) for the 6613 Å absorption, one obtains an *E(B-V)* of 0.97 and 1.30 mag, respectively. A mean value of $E(B\text{-}V) = 1.13$ is then adopted, which is also in good agreement with the estimate given by Bailyn et al. (1995a).

All the spectra presented here were thus corrected for the interstellar absorption using this mean value and by applying the prescription of Cardelli et al. (1989). Then, as made in the previous Chapters, the time at mid-exposure of each spectrum was expressed in HJDs.

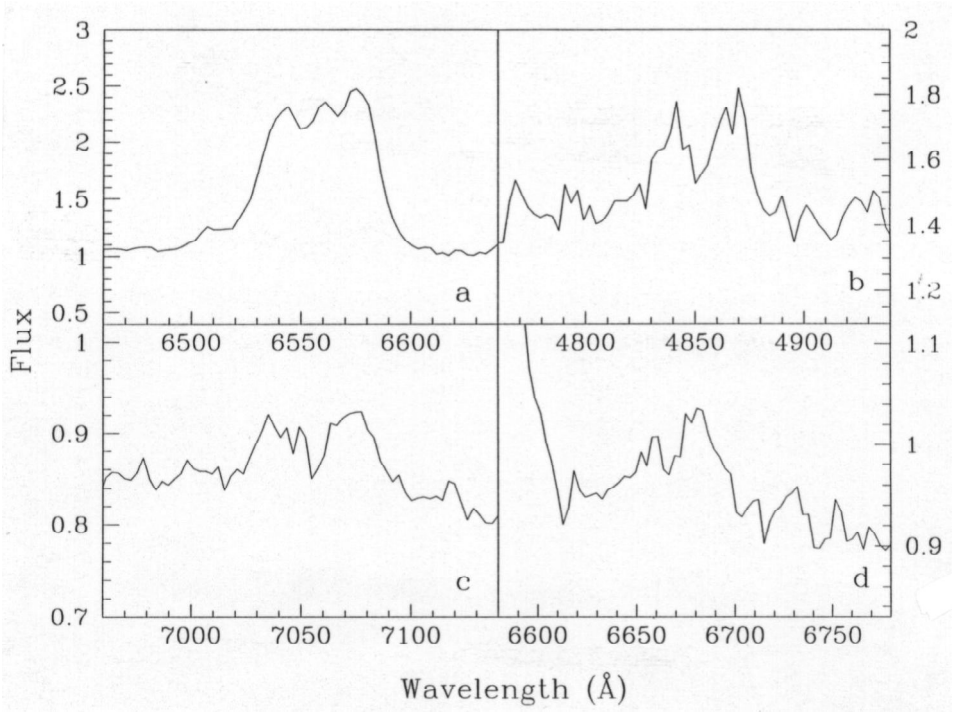

Fig. 6.2a-d. Profiles of **a** Hα, **b** Hβ, **c** He I λ7066 and **d** He I λ6678 emission lines during outburst maximum (August 1994 run). Fluxes are in units of 10^{13} ergs cm^{2} s^{1} $Å^{1}$. Correction for interstellar reddening has been applied.

The mean of the 40 outburst spectra is displayed in Fig. 6.1. The predominant H_α emission and the, fainter, H_β present structured profiles (double- or triple-peaked; Fig. 6.2a,b) while rather noisy H_γ and H_δ components are visible. The emissions of He I λ6678, He I λ7066 (Fig. 6.2c,d, respectively), and possibly He I λ5876 also show double-peaked profiles. The N III λ4640 and the He II λ4686 emissions appear weakly blended.

The single mid-resolution spectrum and the mean of the 12 high-resolution spectra of the X-ray Nova acquired during the decline are presented in Fig. 6.3a,b,

respectively. Unfortunately, the high-resolution mean spectrum of the decline was obtained under non-photometric conditions which did not allow reliable spectrophotometric measurements. Thus it was chosen to plot in Fig. 6.3b the mean of the 12 high-resolution spectra normalized to the continuum.

Table 6.II reports the EWs of the main emission lines for the outburst and the decline mean spectra.

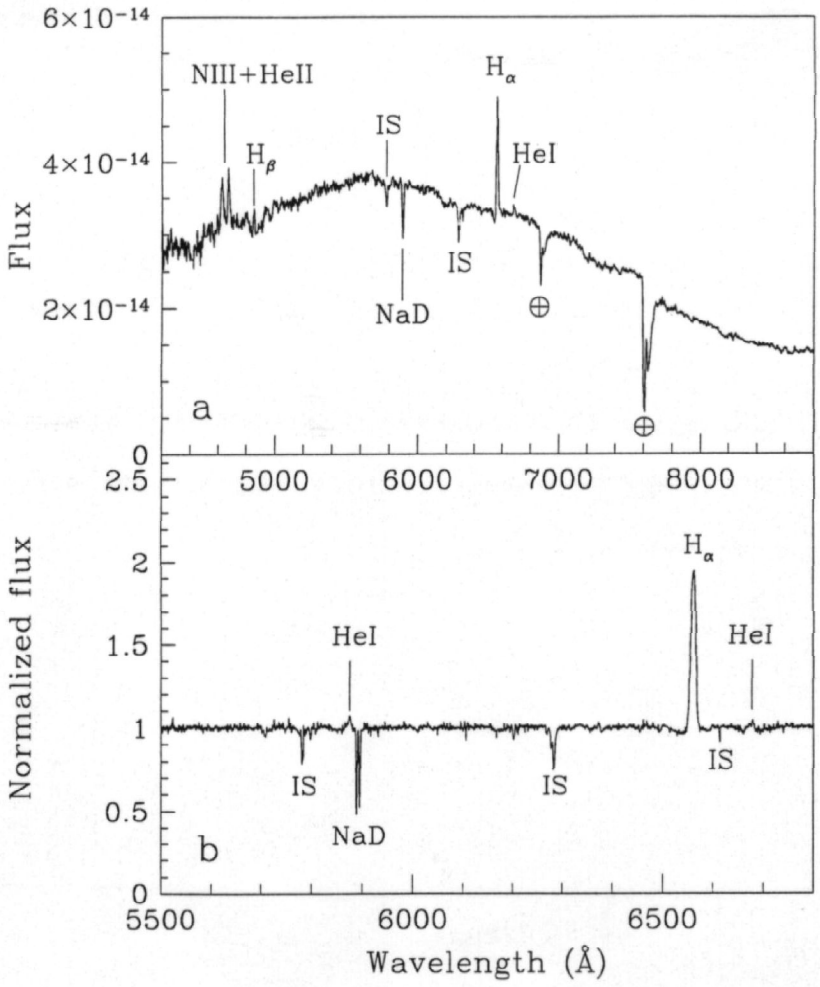

Fig. 6.3. a Mid-resolution spectrum of GRO J1655-40 taken on March 3, 1995. **b** Mean of 12 high-resolution spectra taken on March 3-4, 1995 normalized to the continuum. The main features are indicated and described in the text. The fluxes given in the upper panel are in ergs cm^{-2} s^{-1} $Å^{-1}$ and are corrected for interstellar reddening.

The fluxes of the continuum and of the emission lines of the outburst spectra of GRO J1655-40 show fluctuations up to 50% of their mean values. The presence of periodic behaviours was investigated by means of the DFT algorithm and of the *CLEAN* approach (Roberts et al. 1987).

A spline fit of the continuum of the 40 outburst spectra between 4000 and 9000 Å was then performed and the variations of its integrated flux (i.e. excluding the emission lines) were studied. The DFT spectrum of the integrated flux of the continuum is given in Fig. 6.4a. A main peak at 0.582623 days, with side aliases at 0.366797 and 1.415528 days, is suggested and confirmed by the *CLEAN* procedure.

Table 6.II. Mean EWs of emission lines present in the outburst and the decline spectra of GRO J1655-40. The Hβ line in the decline spectra seems to be formed by a shallow absorption (abs) plus a narrow emission core.

Emission line	Outburst EW (in Å)	Decline EW (in Å)
Hα	68.4	6.45
Hβ	7.39	1.16 (9.28 abs.)
Hγ	7.28	——
Hδ	5.07	——
He I λ5876	3.76	0.73
He I λ6678	1.98	0.65
He I λ7066	4.65	——
He II λ4686	5.30	3.85
N III λ4640	5.88	4.59

The DFT of the fluxes of Hα emission line shown in Fig. 6.4b presents a main peak at 1.296807 days. This period is also suggested by the *CLEAN* algorithm and by the Sterken's (1977) best-fit method. It may be noted that this value is almost exactly half the period of the radial velocity curve found by Bailyn et al. (1995b). This peak of the DFT coincides within the errors with the 1.42 days alias of the DFT of the continuum. Other relevant aliases of the Hα line flux DFT fall at 4.24 days and 0.56 days.

The fluxes of the other emission lines show rather noisy DFT power spectra. Main peaks are found at 0.270 days for Hβ and for He I λ7066, and at 0.213 days for He II λ6678. One can however note that all of these peaks belong also to the sequence of aliases of the DFTs of the continuum and of the Hα line fluxes (Figs. 6.4a and 6.4b, respectively).

The DFTs of the EWs of the sum of all the emission lines, including Hα, do not suggest any periodicity, being dominated by the pure data sampling.

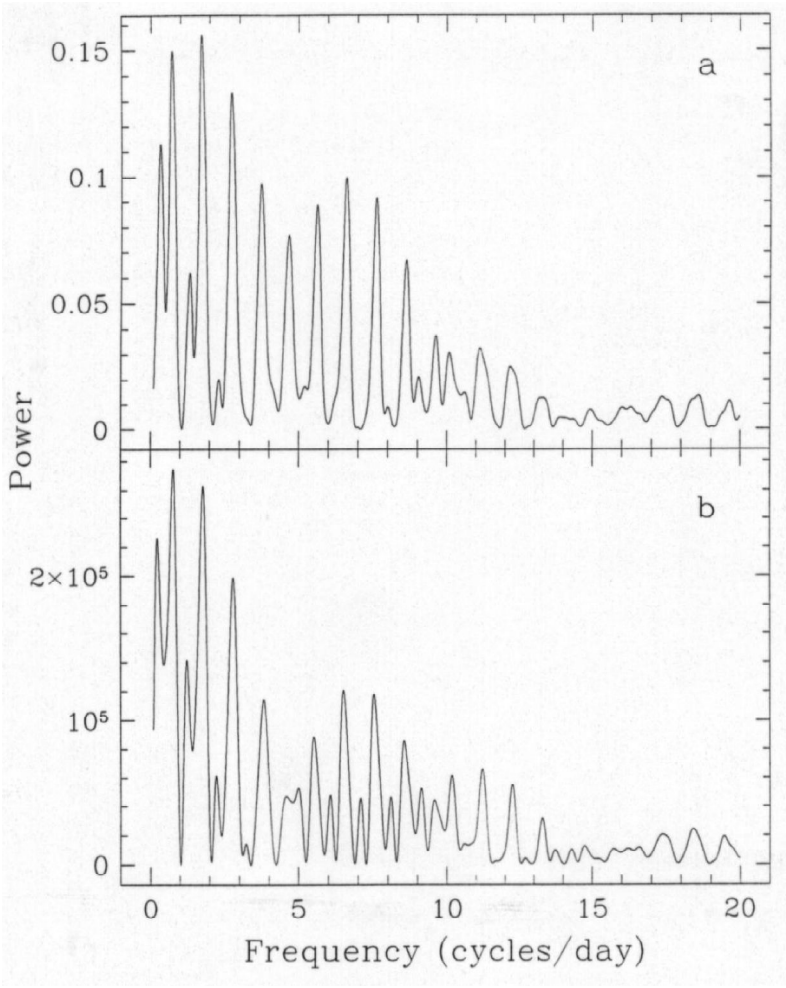

Fig. 6.4. DFTs of **a** 4000-9000Å continuum and **b** Hα emission line fluxes (both are not corrected for interstellar reddening) during the August 1994 run. The peak of the peaks falls at 0.583 days (with a 1-day alias at 1.415 days) for the continuum, and at 1.297 days for Hα. The DFTs of Hβ, He I λ6678 and He I λ7066 show the same sequence of aliases of the continuum, though the main peaks of their DFT fall at higher frequencies (see text).

As remarked before, on August 17 1994, Bailyn et al. (1995a) observed a vatiation in the light curve of GRO J1655-40 likely due to an eclipse. According to the ephemeris given by Bailyn et al. (1995b), this event could correspond to the eclipse of the secondary star by the disk, although the behaviour of the *V-I* color index observed by Bailyn et al. (1995a) seems to indicate lower temperatures inside the eclipse. The last three spectra of the August 14, 1994 run should then fall at the beginning of a secondary eclipse, the one immediately before that observed by Bailyn et al. (1995a). Indeed one can observe that the fluxes of the continuum and the emission lines of these three spectra show a sudden decrease with respect to those of the same night. These data points will be represented in the folded light curves of Figs. 6.6 and 6.7 with open circles.

Then, harmonic analysis of the August 1994 data after the exclusion of the eclipse points was attempted. It was noted that the DFTs of the fluxes of H_α and of the continuum are now more similar to each other, as shown in Fig. 6.5a,b. A most probable modulation at 1.3 days is indicated (and confirmed by the *CLEAN* approach), although, in this case, the 'odd' sequence of the 1-day aliases of the DFT of results stronger than the 'even' sequence. This effect is however mainly due to the sampling. Indeed, if one subtracts from the fluxes the 1.3 days modulation, one obtains a pure noise DFT.

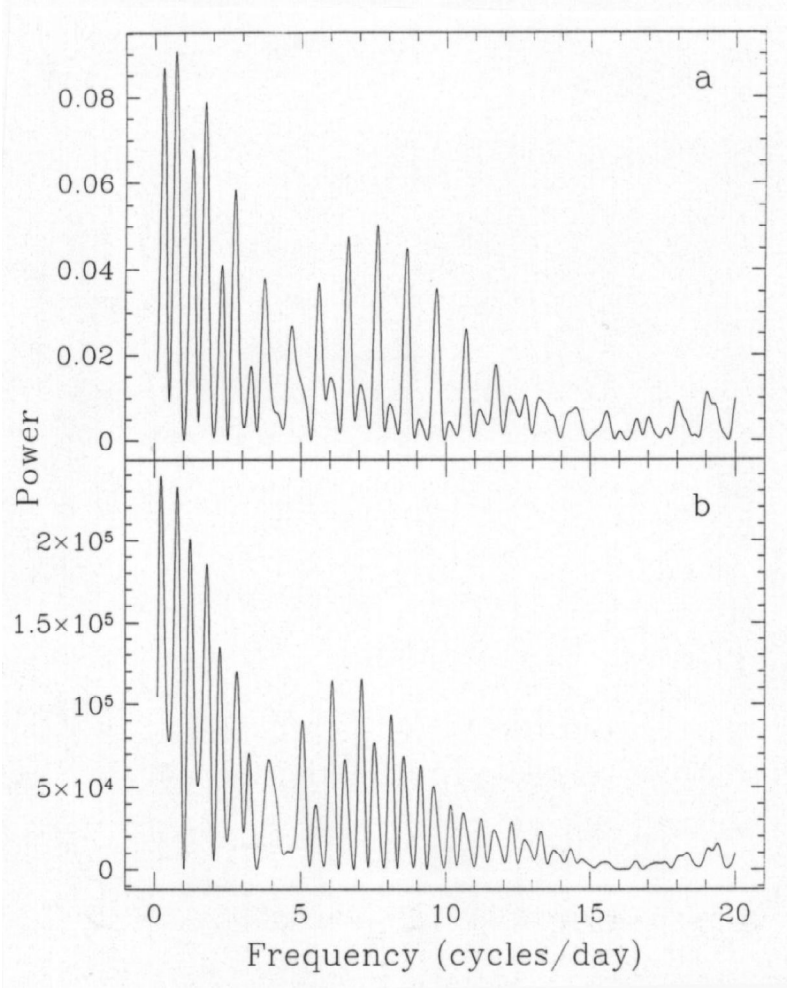

Fig. 6.5. The same as Fig. 6.4 but without taking into account the eclipse data points. The sequence of aliases of the continuum and of the Hα fluxes are now very similar. The main peak of the DFT of the continuum fluxes falls at 1.297 days.

The DFTs of He I and He II emissions are similar to those obtained using the full data sets, with peaks that still belong to the sequence of the aliases found for H_α and for the continuum. In this case, periods longer and shorter than the 1.3 days modulation would be suggested by He I and He II lines, respectively. If one however

subtracts a 1.3 days cosinusoidal signal with appropriate amplitude and phase from the He I and He II data sets, DFTs are obtained which show lower level peaks falling at ≈0.15 and at ≈0.45 days, respectively, which still are aliases of the 1.3 days period. Instead, the He II/He I flux ratios show no signal at all above the noise level, thus suggesting quite similar behaviours in the modulation of these two sets of lines.

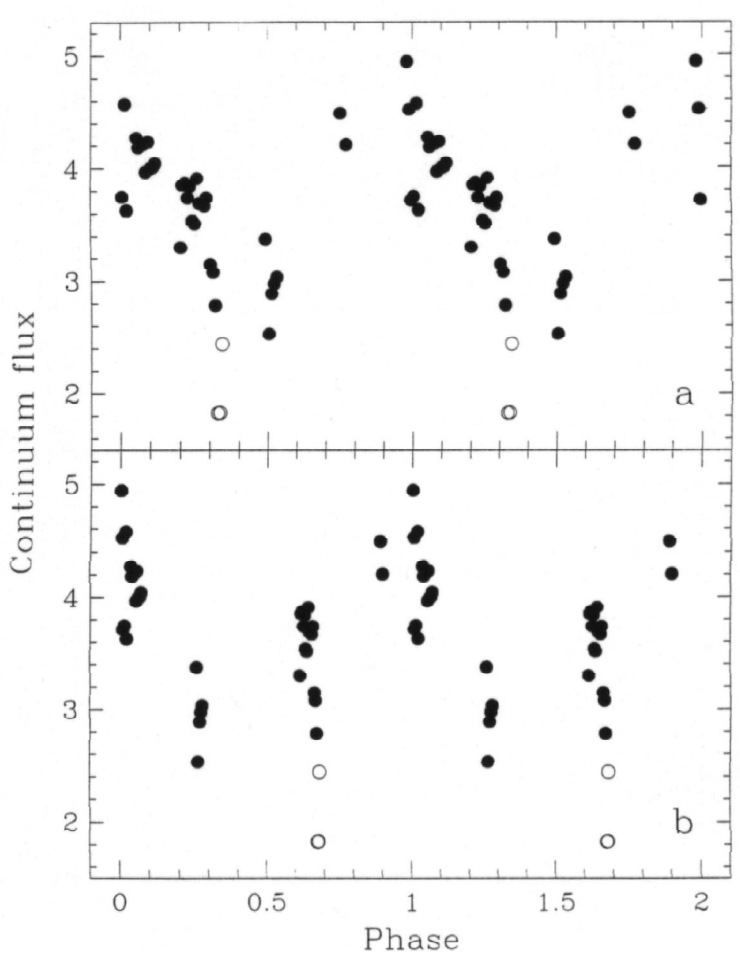

Fig. 6.6. Light curve of the continuum flux (4000÷9000 Å) at light maximum (August 1994 observations) folded with **a** the 1.3-day modulation found here and **b** Bailyn et al.'s (1995b) 2.6-day periods (see text). Phases are arbitrarily referred to HJD=0.00. Fluxes are in units of 10^{-11} ergs cm^{-2} s^{-1} and are not corrected for interstellar reddening. Open circles refer to a possible beginning of an eclipse.

Also, it is noteworthy the fact that the values of the EWs of all emission lines show no significant modulation.

The light curves of the integrated continuum folded with the 1.3 and the 2.6 days periods (the former being the main modulation found for H_α, and the second the radial velocity curve periodicity found by Bailyn et al. 1995b) are shown in Fig. 6.6a,b,

respectively. The fluxes of H_α emission line folded with the 1.3 and 2.6 days periods are given in Fig. 6.7a,b, respectively.

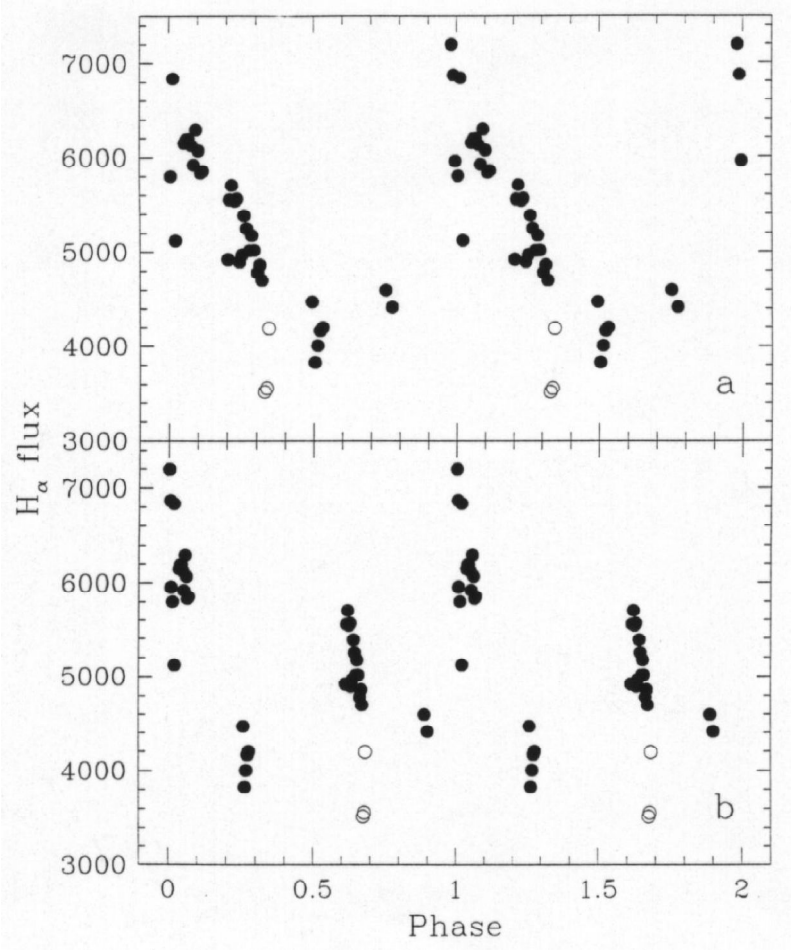

Fig. 6.7. Light curve of the Hα emission line flux during maximum (August 1994 observatons) folded with **a** the 1.3-day modulation found here and **b** Bailyn et al.'s (1995b) 2.6-day period (see text). Phases are arbitrarily referred to HJD=0.00. Fluxes, in units of 10^{-16} ergs cm^{-2} s^{-1}, are not corrected for interstellar reddening. Open circles refer to a possible beginning of an eclipse.

Multi-varied analysis has been also performed on the EWs and the fluxes of the main emission lines and on the continuum fluxes of the August 1994 spectra in order to look for correlations between these quantities. The eclipse data points have been excluded. The linear correlation coefficients between each couple of relevant values are reported in Table 6.III, as well as (in parentheses) their corresponding probability to be higher in the case of a random sample of observations taken from an uncorrelated parent population (see Appendix C-3 of Bevington 1969).

As one can notice, the analysis suggests strong correlation between the fluxes of the H_α line and of the continuum. Both quantities appear instead only weakly

correlated with all the other emission lines, included Hβ. Almost no correlation is found between the fluxes and the EWs of the lines, with the exception of He I and He II. The correlation coefficients between the EWs are also quite low.

Table 6.III. Correlation coefficients obtained with multi-varied analysis performed over EWs and fluxes of the most prominent emission lines and over the flux of the continuum of the August 1994 spectra and, between parentheses, their corresponding probability to be higher in the case of a random sample of observations taken from an uncorrelated parent population. The eclipse points were excluded from these computations.

	F_{cont}	F_{H_α}	F_{H_β}	$F_{He\ I}$	$F_{He\ I}$	EW_{H_α}	EW_{H_β}	$EW_{He\ I}$	$EW_{He\ II}$
F_{cont}	—	0.82 (0%)	0.46 (0.4%)	0.21 (20%)	0.28 (10%)	-0.23 (18%)	-0.22 (20%)	0.33 (5%)	-0.24 (15%)
F_{H_α}	0.82 (0%)	—	0.38 (2%)	0.16 (35%)	0.30 (8%)	-0.10 (70%)	-0.12 (45%)	0.18 (30%)	-0.09 (80%)
F_{H_β}	0.46 (0.4%)	0.38 (2%)	—	0.50 (0.2%)	0.44 (0.5%)	-0.14 (40%)	0.25 (15%)	0.15 (40%)	0.09 (80%)
$F_{He\ I}$	0.21 (20%)	0.16 (35%)	0.50 (0.2%)	—	0.41 (1%)	-0.16 (35%)	0.00 (100%)	0.79 (0%)	0.19 (25%)
$F_{He\ II}$	0.28 (10%)	0.30 (8%)	0.44 (0.5%)	0.41 (1%)	—	0.07 (85%)	0.06 (90%)	0.15 (40%)	0.57 (0%)
EW_{H_α}	-0.23 (18%)	-0.10 (70%)	-0.14 (40%)	-0.16 (35%)	0.07 (85%)	—	0.04 (100%)	-0.05 (95%)	0.08 (80%)
EW_{H_β}	-0.22 (20%)	-0.12 (45%)	0.25 (15%)	0.00 (100%)	0.06 (90%)	0.04 (100%)	—	0.06 (90%)	0.34 (4%)
$EW_{He\ I}$	0.33 (5%)	0.18 (30%)	0.15 (40%)	0.79 (0%)	0.15 (40%)	-0.05 (95%)	0.06 (90%)	—	0.33 (5%)
$EW_{He\ II}$	-0.24 (15%)	-0.09 (80%)	0.09 (80%)	0.19 (25%)	0.57 (0%)	0.08 (80%)	0.34 (4%)	0.33 (5%)	—

Finally, no noticeable result came out from the DFT analysis of the variations of the peak-to-peak separations and of the V/R ratio between the fluxes of the blue and red components of the double-peaked emission lines.

6.4. DISCUSSION

Only few SXTs, such as GRO J1655-40, have been systematically monitored throughout the whole decline. The presence of X-ray minioutbursts during the decline (Zhang et al. 1995) with a recurrence time of 120 days reminds the light curve of the other SXT V518 Per (=GRO J0422+32), which presented **the same** periodicity in the

secondary outbursts, although this object appeared more active in the optical than in the X-ray (Chevalier & Ilovaisky 1995).

The binary nature of GRO J1655-40 was assessed by the photometric study of Bailyn et al. (1995a). One of he peculiarities of this object, amongst the other SXTs, is the presence of structured radio jets; this supports the hypothesis of mass accretion onto a collapsed primary harbored inside a highly inclined binary system (Hjellming & Rupen 1995, Tingay et al. 1995).

6.4.1. Spectral evolution of the outburst

The decrease of the continuum flux during the decline (Fig. 6.3a) is consistent with the observed brightness magnitude difference of ≈2 magnitudes between the August 1994 and the March-April 1995 *V*-band luminosities of the system observed by Bailyn et al. (1995a, 1995b). The spectrum of Fig. 6.3a was obtained when the star was about one magnitude above its light minimum, located at $V \sim 17.3$ (Bailyn et al. 1995a). It shows a solar-like energy distribution which would then appear slightly cooler than that of the intermediate F-type suggested by Bailyn et al. (1995b) for the secondary star. This difference could however be due to inaccurate flux calibration of the spectrum reported in Fig. 6.3a.

During the decline, the intensity of the H_α emission has faded by a factor ≈25, while the flux of the integrated continuum between 5500 and 6750 Å reduced only by a factor ≈5 - 6. Table 6.II shows that an analogous decrease of its EW is presented also by the H_β emission, while smaller changes are observed in the emissions of He I λ6678, N III λ4640, He II λ4686 and He I λ5876 in this phase. This fact indicates that the line emitting region of GRO J1655-40 shrinks more steeply than that of outbursting DNe.

This represents a basic difference between the behaviours of SXTs and DNe. In DNe, Balmer emission lines appear weaker at light maxima, and well inside shallow absorption components; then, as the object evolves towards light minimum, the absorption wings disappear and the emission components strengthen considerably.

The opposite trend observed in SXTs (e.g. Bailyn & Orosz 1995 for MM Vel; Callanan et al. 1995 for V518 Per) supports the idea that during their outbursts a strong increase **also of the mass transfer rate from the secondary**, and not only through the disk, is produced, most probably by the X-ray heating of the secondary itself by the primary (see Sect. 3.4 of this Thesis). The bulk of the line emission region could then be placed in the gas stream between the two components.

One also notes that in GRO J1655-40 the full width at zero intensity (FWZI) of H_α emission is ~120 Å at light peak, and only ~30 Å during the decline, when profiles are no longer double peaked and resemble more those of Nova-Like objects. This indicates the presence in the line-emitting region of large velocity fields (up to about ±2700 km s^{-1}) near the light peak, and of lower velocities (up to about ±700 km s^{-1}) at light minimum. This explains why one can see the ~100 Å wide absorption around the H_α and H_β emissions only in the decline spectra, when the emission components are narrower. One may also note that the velocity fields observed in SXTs are generally larger then those observed in DNe, thus supporting the existence in the former ones of rather massive primaries.

The mean peak-to-peak half separation of the H_α emission profile at light maximum might indicate keplerian velocities of ≈800 km s^{-1}. The full width at half maximum (FWHM) of the single-peaked H_α in the decline spectra is instead ~17 Å, suggesting rotational velocities of ≈400 km s^{-1}. If one assumes a 5.4 $M_\odot$ primary (Bailyn et al. 1995b), and a orbital inclination $i \approx 90°$, the radius of the accretion disk in outburst is ~1.6 $R_\odot$, that is only 0.25 times the Roche lobe radius of the primary, but it reaches the radius of the Roche lobe during the decline. This behaviour is once again opposite to that displayed by outbursting DNe, the accretion disks of which, as a consequence of the disk instability mechanism, present larger radii at light maximum than at quiescence. In SXTs, instead, in addition to the disk instability phenomenon, a strong increase of the mass transfer rate from the X-ray heated secondary is observed. Such a burst of low angular momentum material from the secondary would then cause the shrinking of the disk in the first phases of the outburst, in particular if (as will be

shown in Ch. 7) the maximum X-ray luminosity of the outburst is not higher than ~10^{38} erg s^{-1}.

6.4.2. Shorter term flux modulations

Since the outburst phase data set presented here spans only over 4 nights (August 12-15, 1994), it is not possible to properly sample the orbital period of 2.6 days found by Bailyn et al. (1995b). Fourier analysis of the fluxes of the main emission features and of the continuum give rather noisy power spectra. Both the fluxes of H_α emission and of the continuum appear to be modulated with a period of 1.297 days, which, within the uncertainties, can be interpreted as being half of Bailyn et al.'s (1995b) spectroscopic period. The DFTs of the fluxes of the other emission lines suggest different main peaks, which are however aliases of the 1.3 days peak.

Actually, Table 6.III shows strong correlations between the fluxes of H_α emission line and those of the continuum and only weaker correlations with the fluxes of the other emission lines. One also finds that the fluxes of the lines are poorly correlated with the EWs, with perhaps the exception of He I and He II.

Unfortunately, the paucity of the data, the sampling effects due to the poor coverage of the suggested orbital period, the presence of strong flickering, interpreted by Bailyn et al. (1995b) as due to disk effects, make difficult any further detailed analysis of short-term modulations during outburst.

6.4.3. The model

As already pointed out before, the behaviour of GRO J1655-40 during the outburst is, like other SXTs, opposite to that of DNe. Indeed, during the peak of the outburst the accretion disk seems to be powered by a stronger flux of material from the secondary. Since the flow is formed by matter with low angular momentum, the disk will tend to have a smaller radius and higher density and temperature during outburst than at quiescence. This explains the larger width of the emission lines observed at

light maximum, when higher keplerian velocities of the outer region of the disk are expected.

The detection of half of the orbital period in the fluxes of the continuum and of the H_α emission line might suggest that similar physical conditions can be observed from two opposite sides of the close binary system. The two equivalent sides of the system might correspond to the two stars being in quadrature with respect to the observer. The maximum flux of the emission lines (mainly H_α) might then be produced in the gas stream and the splash region, or the hot spot, placed on the outer edge of the disk. One must however however note that: (a) the half orbital period modulation is observed also in the continuum flux, while almost no modulation is observed in the EWs of all the emission lines; (b) no periodic modulation is seen in the ratio of the fluxes of He II and He I emission lines. This means that: (a) the observed variations throughout the orbital cycle are mainly due to geometrical reasons and not only to changes in the volume of the line emitting region; (b) no modulation of the temperature of the line emitting region is observed.

These facts may be explained either by an asymmetry of the disk shape or by the presence of some vertically extended structure on the disk itself corotating with the binary system.

Anyway, the splash region created by the stream impacting the outer edge of the disk might result in a quite extended optically thick curtain of gas. This curtain should then be heated by the UV and X-ray flux from the central object and produce eclipses. Such a structure might be visible from two opposite directions.

Moreover, an optically thick gas layer might perhaps explain the shape of the eclipse light curve of GRO J1655-40 (Fig. 6.8, from Bailyn et al. 1995b). This figure in fact shows that:

1) primary and secondary minima are equidistant;
2) the profile of the main eclipse is asymmetric, the decline being less steep than the rise;

3) the width of the main eclipse is unusually large, the decline starting at ~0.35 × P_{orb} before the minimum, while the eclipse ends at ~0.25 × P_{orb} after the minimum.

The curtain produced by splashed gas could then contribute to widen the declining part of the eclipse light curve.

The remarkably large width of the main eclipse could also be explained by hypothesizing that during the decline the outer parts of the accretion disk undergo considerable expansion up to the radius of the Roche lobe.

From the depths of the two eclipse minima one can also infer that, during the decline, the secondary contributes to the total luminosity in the *V* band for about one half of the disk luminosity.

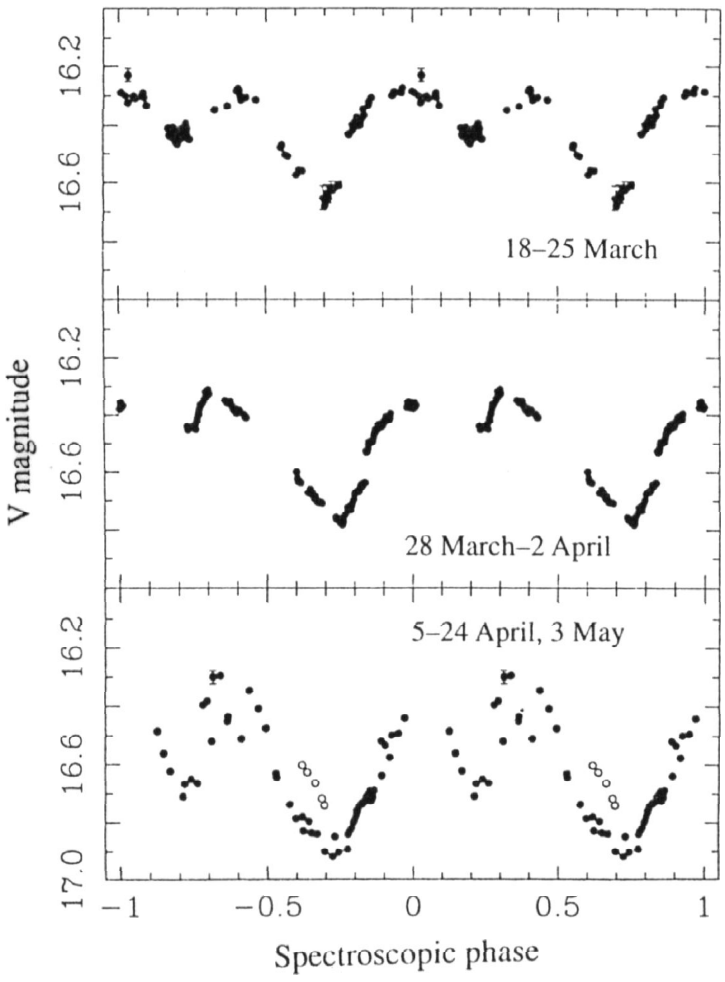

Fig. 6.8. *V*-band light curves of GRO J1655-40 folded with a period of 2.612 days. Note the remarkable width of the primary eclipse (from: Bailyn et al. 1995b).

During the outburst phase, the splashed material can continue its trajectory flowing above and below the disk and finally fall onto the disk at about the circularization radius. This would produce optically thick blobs of material which orbit inside the disk at keplerian velocities.

Light modulations with period shorter than the orbital one have been observed during the high states of activity of several SXTs, like e.g. V404 Cyg (Gotthelf et al. 1992) and GRS 1009-45 (Bailyn & Orosz 1995). In the case of the SXT V2293 Oph such variations were interpreted by Masetti et al. (1996; see also Ch. 4 of this Thesis) as the effect of blobs orbiting in the inner region of the disk. On the contrary, no clear evidence of short-term periodicities was found in GRO J1655-40. A rather flickered light curve has been however observed. As suggested by Bailyn et al. (1995b), the activity in the disk, such as X-ray heating, hot spots and/or superhumps, might complicate the optical light curve of this X-ray Nova producing non-regular fluctuations.

REFERENCES OF CHAPTER 6

- Alexandrovich N., Borozdin K., Sunyaev R.A., 1995, IAU Circ. 6143
- Bailyn C.D., Orosz J.A., 1995, ApJ, 440, L73
- Bailyn C.D., Orosz J.A., Girard T.M. et al., 1995a, Nat, 374, 701
- Bailyn C.D., Orosz J.A., McClintock J.E., Remillard R.A., 1995b, Nat, 378, 157
- Bevington P.R., 1969, Data reduction and error analysis for the physical sciences. McGraw-Hill Book Company, New York
- Brandt W.N., Podsiadlowski P., Sigurdsson S., 1995, MNRAS, 277, L35
- Callanan P.J, Garcia M.R., McClintock J.E. et al., 1995, ApJ, 441, 786
- Cardelli J.A., Clayton G.C., Mathis J.S., 1989, ApJ, 345, 245
- Chevalier C., Ilovaisky S.A., 1995, A&A, 297, 103
- Crary D.J., Kouveliotou C., van Paradijs J. et al., 1996, ApJ, 463, L79
- Della Valle M., Dürbeck H.W., 1993, A&A, 275, 239
- Gotthelf E., Halpern J.P., Patterson J., Rich R.M., 1992, AJ, 103, 219
- Harmon B.A., Wilson C.A., Zhang S.N. et al., 1995a, Nat, 374, 703
- Harmon B.A., Zhang S.N., Fishman G.J. et al., 1995b, IAU Circ. 6128
- Harmon B.A., Zhang S.N., Paciesas W.S., Fishman G.J., 1995c, IAU Circ. 6147
- Harmon B.A., McCollough M.L., Zhang S.N., Paciesas W.S., Wilson C.A., 1995d, IAU Circ. 6196
- Harmon B.A., Paciesas W.S., Fishman G.J., 1995e, IAU Circ. 6205
- Harmon B.A., Wilson C.A., McCollough M. et al., 1996a, IAU Circ. 6436
- Harmon B.A., Robinson C.R., Fishman G.J., Zhang S.N., Paciesas W.S., 1996b, IAU Circ. 6501
- Herbig G.H., 1975, ApJ, 196, 129
- Hjellming R.M., Rupen M.P., 1995, Nat, 375, 464
- Horne K., Harlaftis E.T., Baptista R. et al., 1996, IAU Circ. 6406
- Hunstead R., Campbell-Wilson D., 1996, IAU Circ. 6410
- Masetti N., Bianchini A., Bonibaker J., Della Valle M., Vio R., 1996, A&A, 314, 123 *(Chapter 4 of this Thesis)*
- Meier D., 1996, ApJ, 459, 185
- Orosz J.A., Schaefer B., Barnes S., 1995, IAU Circ. 6203
- Remillard R.A., Bradt H., Cui W. et al., 1996, IAU Circ. 6393
- Roberts D.H., Lehár J., Dreher J.W., 1987, AJ, 93, 968
- Sazonov S., Sunyaev R.A., 1995a, IAU Circ. 6201
- Sazonov S., Sunyaev R.A., 1995b, IAU Circ. 6209
- Sterken C., 1977, A&A, 57, 361
- Tingay S.J., Jauncey D.L., Preston R.A. et al., 1995, Nat, 374, 141
- Wilson C.A., Harmon B.A., Zhang S.N. et al., 1994, IAU Circ. 6056
- Wilson C.A., Harmon B.A., Zhang S.N., Paciesas W.S., Fishman G.J., 1995, IAU Circ. 6152
- Zhang S.N., Wilson C.A., Harmon B.A. et al., 1994, IAU Circ. 6046
- Zhang S.N., Harmon B.A., Paciesas W.S., Fishman G.J., 1995, IAU Circ. 6209